http://doi.org/10.35784/iapgos.5903 *received: 17.02.2024 | revised: 12.05.2024 | accepted: 19.06.2024 | available online: 30.06.2024*

IDENTIFICATION OF SALT-AFFECTED SOILS IN THE COASTAL AREA OF KRISHNA DISTRICT, ANDHRA PRADESH, USING REMOTE SENSING DATA AND MACHINE LEARNING TECHNIQUES

Govada Anuradha, Venkata Sai Sankara Vineeth Chivukula, Naga Ganesh Kothagundla
V. R. Siddhartha Engineering College, Faculty of Department of Computer Science and Engineering, Vinobha Nagar, Ibrahimpatnam, India

Abstract. *In agricultural soil analysis, the challenge of soil salinization in regions like Krishna District, Andhra Pradesh, profoundly impacts soil health, crop yield, and land usability, affecting approximately 77,598 hectares of land. To address this issue, three machine learning algorithms are compared for classifying salinity levels in the coastal area of Krishna district, Machilipatnam. This study utilizes Landsat-8 images from 2014 to 2021, correcting for cloud cover and creating a true-color composite. The study area is defined and visualized. Twelve indices, derived from Landsat imagery, are incorporated into the analysis. These indices, including spectral bands and mathematical expressions, are added as image bands. The median of these indices is calculated, and sample points representing both non-saline and saline areas are used for supervised machine learning. The data is divided into two sets: training and validation. The study evaluates Random Forest, Classification and Regression Trees, and Support Vector Machines for classifying soil salinity levels using these indices. The RF algorithm produced an accuracy of 92.1%, CART produced 91.3%, and SVM produced 86%. Results are displayed on the map, representing predicted salinity levels with distinct colors. Performance metrics are evaluated, and they assess algorithm performance. The research involved gives insights into the classification of soil salinity using machine learning, which could represent an efficient solution to the problem of soil salinization in Machilipatnam.*

Keywords: soil salinity, salinity index, remote sensing, machine learning, prediction

IDENTYFIKACJA GLEB ZASOLONYCH W STREFIE PRZYBRZEŻNEJ DYSTRYKTU KRISHNA, ANDHRA PRADESH, Z WYKORZYSTANIEM DANYCH TELEDETEKCYJNYCH I TECHNIK UCZENIA MASZYNOWEGO

Streszczenie. *W rolniczej analizie gleby, wyzwanie zasolenia gleby w regionach takich jak dystrykt Krishna, Andhra Pradesh, głęboko wpływa na zdrowie gleby, plony i użyteczność gruntów, wpływając na około 77 598 hektarów ziemi. Aby rozwiązać tę kwestię, porównano trzy algorytmy uczenia maszynowego do klasyfikacji poziomów zasolenia w obszarze przybrzeżnym dystryktu Krishna, Machilipatnam. W badaniu wykorzystano obrazy Landsat-8 z lat 2014-2021, korygując je pod kątem zachmurzenia i tworząc kompozycję w prawdziwych kolorach. Obszar badań został zdefiniowany i zwizualizowany. Do analizy włączono dwanaście wskaźników pochodzących ze zdjęć Landsat. Wskaźniki te, w tym pasma widmowe i wyrażenia matematyczne, są dodawane jako pasma obrazu. Mediana tych wskaźników jest obliczana, a przykładowe punkty reprezentujące zarówno obszary niezasolone, jak i zasolone są wykorzystywane do nadzorowanego uczenia maszynowego. Dane są podzielone na dwa zestawy: treningowy i walidacyjny. W badaniu oceniono Random Forest, Classification and Regression Trees i Support Vector Machines pod kątem klasyfikacji poziomów zasolenia gleby przy użyciu tych wskaźników. Algorytm RF uzyskał dokładność 92,1%, CART 91,3%, a SVM 86%. Wyniki są wyświetlane na mapie, przedstawiając przewidywane poziomy zasolenia za pomocą różnych kolorów. Oceniane są wskaźniki wydajności i wydajność algorytmów. Przeprowadzone badania dają wgląd w klasyfikację zasolenia gleby przy użyciu uczenia maszynowego, co może stanowić skuteczne rozwiązanie problemu zasolenia gleby w Machilipatnam.*

Słowa kluczowe: zasolenie gleby, wskaźnik zasolenia, teledetekcja, uczenie maszynowe, przewidywanie

Introduction

Raising the salt content of the soil is a process known as soil salinization, which hinders plant growth and causes the land to deteriorate. The region's economy, farmers' well-being, and agricultural output are all negatively impacted by saline soils. Several reasons might lead to soil salinization, including dry climates, irrigation, inadequate drainage, and rising sea levels. Water absorption is mainly impacted by soil salinity on plant growth. Crops cannot absorb enough water to survive, even when the soil is sufficiently moist. Soils contaminated by salt are becoming a global issue [5]. It is regarded as a significant barrier to increasing agricultural output to feed the world's expanding population. Worldwide, salt-affected soils (SAS) affect around 1125 million hectares of land, of which humans cause 76 million hectares [15]. 6.74 million hectares of land in India have soils contaminated by salt [22].

2.956 m ha of saline soil and 3.77 m ha of sodic soil make up India's 6.727 m ha (2.1% of the country's total geographical area) of salt-affected land (SAL) [7]. Due to soil salinization, the nation loses 16.84 million tons of agricultural output yearly, at Rs 230.20 billion [24]. Andhra Pradesh state has approximately 0.6 m ha of SAS, which also comprise both saline and sodic soils [24]. Andhra Pradesh state has approximately 0.6 m ha of SAS, which also comprise both saline and sodic soils [8]. The rising sea level and changing climate may accelerate soil salinization, making developing countries with high population densities more vulnerable than other areas.

According to Zhu [34], salinity and high alkalinity harm soil fertility, damaging the land and making it harder for plants to thrive. Due to the challenging climate, soil salinity is vital in semi-arid locations, mainly when food and fiber are in short supply [16]. It has been shown that the conventional approach of gathering soil samples and analyzing them in a lab afterward needs to be revised and appropriate to meet the rate of development of this phenomenon, particularly given how expensive, time-consuming, and challenging it is to update these methods.

Soil salinity maps have been created using more remote sensing data and techniques. Globally, a great deal of study has been done during the past three decades on mapping soil salinity using satellite photos. Soil salinity may now be accurately and promptly assessed at various locations and times because of the development of satellite data availability and analysis capabilities. Based on topography data, climatic conditions, land use data, etc., various spatial models have been tested to assess saline soil [12]. Normalized Differential Vegetation Index (NDVI), Generalized Difference Vegetation Index (GDVI), Enhanced Vegetation Index (EVI), Normalized Difference Salinity Index (NDSI), and Salinity Indices (SI), are some of the spectral indices used in soil salinity mappings.

Researchers have employed various machine learning techniques, including Random Forest (RF), Support Vector Machine (SVM), and Classification and Regression Trees (CART). However, they discovered that the RF method was the most accurate of these techniques [31, 33].

1. Literature review

Kabiraj et al. [17] utilized remote sensing techniques to analyze the Land use pattern of SAL. Satellite data from Sentinel-2, Landsat-8, and Landsat-5, plus topographical data from Shuttle Radar Topographical Mission were acquired in 2020, 2015, and 2009. Twenty spectral indices were analyzed, including vegetation indices for drought, soil salinity indices, and topographical characteristics. The researchers applied the RF model to detect SAL, using 593 soil samples for training and validation. The predicted SAL extent in 2020 was 134.4 sq. km using kfold cross-validation with an overall accuracy of 93%. The SAL area increased by 11.6% during the study period. The study has distinguished the role of remote sensing techniques in assessing SAL, which can be the best tool to quantify unproductive lands for reclamation or some other productive utilization.

Kumar et al. [21] described a machine learning-based approach to effectively observe and classify SAS of Raibareli district of Uttar Pradesh, India, comparing three popularly used machine learning techniques: Logistic Regression, SVM, and RF. The authors carried other salinity indices and principal components by analysing of various Landsat 8 OLI/TIRS bands, and they used nearby data such as nearness to canals and streams.

To determine the best satellite image for determining soil salinity based on 5-fold cross-validation, Kabiraj et al. [18] compared Sentinel2 and Landsat-8 data from 2020 in their study to evaluate SAL in West Bengal, India. Using the RF model, the researchers analysed a variety of spectral indices of vegetation and soil salinity.

To map the salinity of soil, Aksoy et al. [2] employed Landsat-8 OLI, Sentinel-2A, ground-based electrical conductivity data, CART, RF, and Support Vector Regression (SVR). With the help of three machine-learning algorithms, one vegetation index, three soil salinity indices, and a wetness band, they produced eight soil salinity maps. They used Information from the ground, Landsat photos, and environmental factors are all considered.

Sentinel-2 Multispectral Imager data and machine learning techniques were utilized by Wang et al. [32] to measure and map soil salinity in arid regions precisely. Three machine learning techniques were used: RF, SVMs, and Artificial Neural Networks (ANN). The research gathered 160 soil-mixed samples, divided them into 30% for verification and 70% for modeling, and then classified them using the K-S algorithm. With an R2 of 0.88, RMSE of 4.89 dS m1, and RPIQ of 1.96, the SVM model fared better than the RF and ANN models regarding accuracy and performance. According to the SVM model's soil salinity mapping, farmland at higher altitudes showed increased salinity caused by prolonged irrigation and secondary salinization. This work provides a scientific justification for simulating dirt.

Through statistical research, Asfaw et al. [3] identified the strongest correlation between the spectral indices and the soil's electrical conductivity (EC) after using Landsat images to produce several spectral indices. They created a single model by combining the EC data from field measurements with the spectral indices seen remotely. They identified places with high soil salinity by using this model to build a salinity map of the research area.

Hoa et al. [14] used five machine-learning models with Sentinel-1 Synthetic Aperture Radar (SAR) C-band data. Gaussian Processes (GP), RF, SVR, Multilayer Perceptron Neural Networks (MLP-NN), and Radial Basis Function Neural Networks (RBFNN) were the models that were employed. Assessing the Mean Absolute Error and Root Mean Square Error was part of the performance evaluation process for the five models.

Rani et al. [26] conducted a study to precisely ascertain the extent of the damaged soils to identify and monitor the affected areas in the Unnao district of Uttar Pradesh, India. The Landsat 8 image bands, different salinity indices calculated from those bands, Digital Elevation Model data, groundwater depth data, proximity to the canal, and MODIS NDVI 16-day composite data have all been subjected to the RF machine learning technique.

2. Proposed methodology

The methodology (Fig. 1) employed in this study consists of three sections aimed at investigating soil salinity in the Machilipatnam region: Study Area, Data Collection and Processing, Selection of Predictors and Modeling.

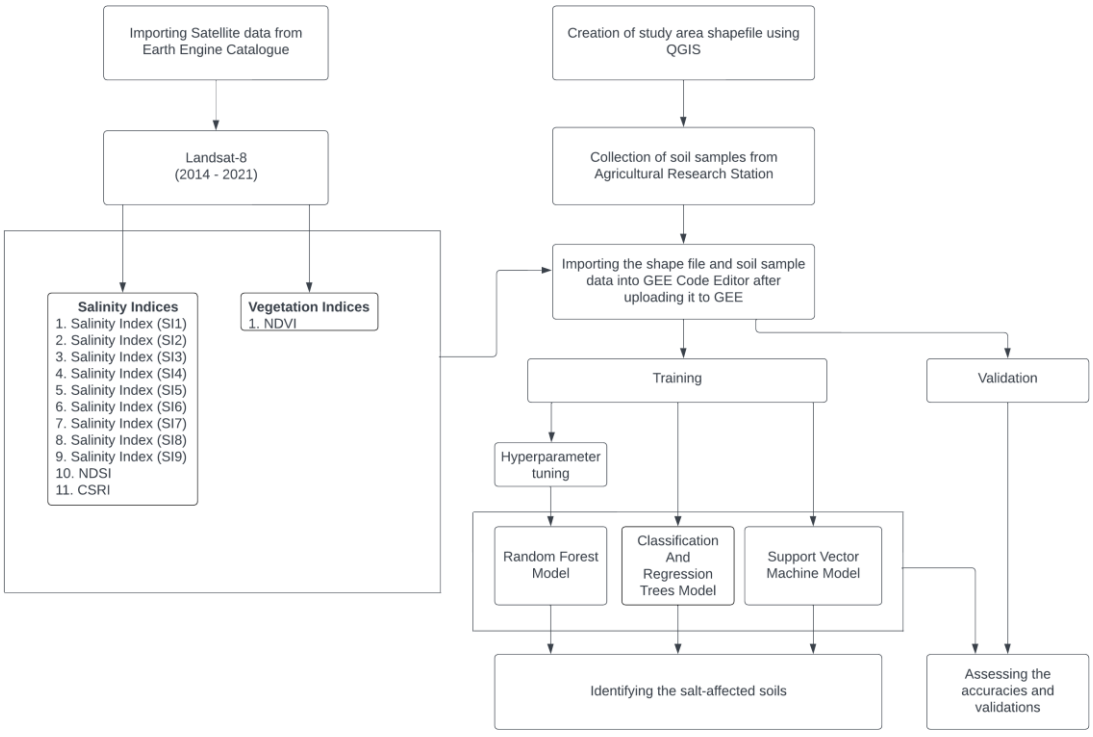

Fig. 1. Methodology for identifying salt-affected soils

2.1. Study area

The study area is Masulipatnam (now Machilipatnam), one of India's ancient coastal towns on the east coast, part of the Krishna district, Andhra Pradesh [25]. It is located at 16°11′ N latitude and 81° 8 ′E longitude [20]. The map of the study area is depicted in Fig. 2. Machilipatnam is notable because it is the location of a prominent magnetic anomaly zone affecting an area of approximately 10,000 square kilometers in the Bay of Bengal [30]. In Machilipatnam, there are five main types of wastelands: salt-affected, coastal, waterlogged/marshy, and barren land types, which can help with groundwater development, agricultural, forestry, and reclamation efforts [23]. Machilipatnam's average yearly temperature ranges from 18 to 32℃, with a higher frequency of around 25℃ [13]. There are four wet and four dry years every 25 years in the Krishna zone of Andhra Pradesh, with an average rainfall of 926.8 mm, with 60% coming from the south-west monsoon and 26% from the north-east monsoon [4].

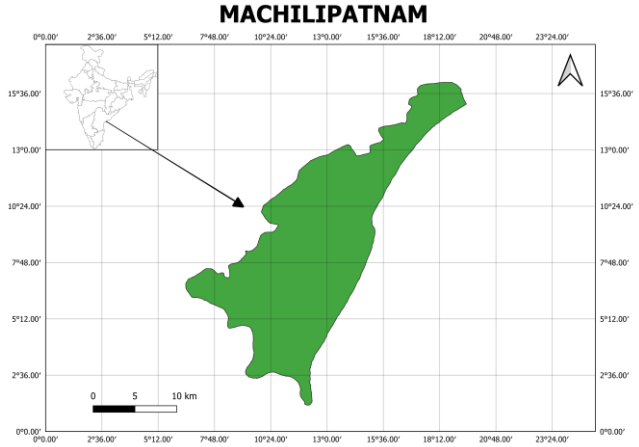

Fig. 2. Study area's location

2.2. Data collection and processing

Fig. 3 provides a general overview of the data collection and processing. The study utilized satellite images of Landsat 8 Collection 2 Tier 1 calibrated top-of-atmosphere (TOA) reflectance obtained from June to September with less than 40% cloud cover from 2014 to 2021, accessible in the Google Earth Engine (GEE).

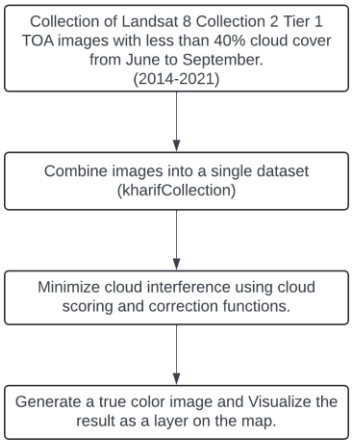

Fig. 3. Flowchart for data collection and processing

Supercomputers are not necessary for users to search, analyze, and visualize large geospatial datasets because of GEE's vast geospatial databases, which include Landsat images and other ready-to-use products. The GEE web application, rapid data processing, and implementation of machine learning algorithms leverage Google's computer infrastructure through an application programming interface library and a development environment that supports Python and JavaScript. The chosen Landsat satellite images were imported from the GEE data library and carefully filtered using various GEE methods in the code editor area. To be more precise, the *ee.ImageCollection.filterDate* was used to separate images taken between June 1st and September 30th, which are the kharif seasons of every year from 2014 to 2021. To minimize atmospheric interference and ensure data quality, images with a cloud cover of more than 40% were excluded using *ee.ImageCollection.filter.Metadata*. With the help of the 'assets' tool and *ee.ImageCollection.filter* in the code editor, the study region defined by a shapefile was quickly included in the analysis and focused on the relevant geographic area. Then, a single dataset called *kharifCollection* was created by combining the merged Landsat collections from every year using *ee.ImageCollection.merge*. Utilizing the *ee.algorithms.Landsat.simple.CloudScore*, which evaluates and modifies the cloud presence in the image, and an image correction function called *applyCorrection* were developed to minimize cloud interference.

The *ee.ImageCollection.map* is then used to apply this adjustment to the previously created Landsat image collection during kharif seasons (i.e., *kharifCollection*), creating a new collection called *correctedCollection*. By choosing the appropriate Landsat bands (B4, B3, and B2) and defining visualization parameters for clarity, the script also sets up a true color composite. A function is developed to clip the corrected images to the designated study area to guarantee that attention is focused on the pertinent geographic area. The final step involves calculating the median of the cropped images and applying the selected visualization parameters to the *Map.addLayer* to show the result as a layer on the map. By generating and showing a cloud-corrected true color composite (Fig. 4) for the study region during the kharif seasons, the complete method makes it feasible to examine the land cover with better clarity and precision. Geometric imports are used for marking the soil samples. There are two types of markings: saline feature collection markings and non-saline feature collection markings based on the collected samples from the soil database.

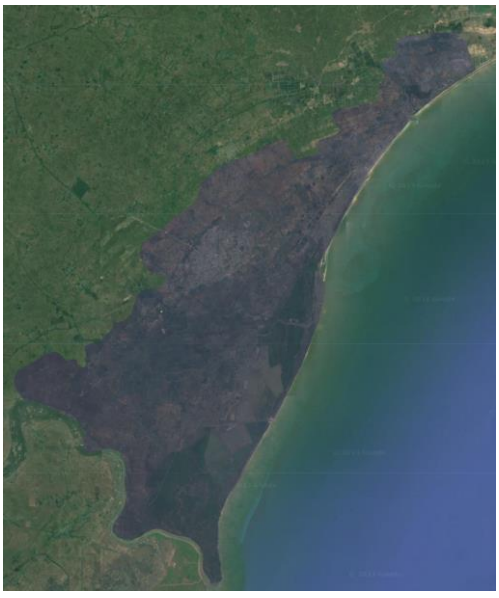

Fig. 4. True Color Image of the study area where clouds are masked

The current study used 430 soil samples in total. These soil samples were acquired from the Agricultural Research Station, Machilipatnam soil database, during the kharif seasons of 2019 and 2020. After generating soil leachate at a soil/water ratio of 1:2.5, the electrical conductivity values of the soil samples were evaluated using a digital multiparameter measuring apparatus. The EC values are classified into two categories: saline (>4 ds/m)

and non-saline (<2 ds/m) [6]. Our study area samples have not encountered any EC values falling within the intermediate range. The points that have been chosen via coordinates from the soil database are shown in Fig. 5.

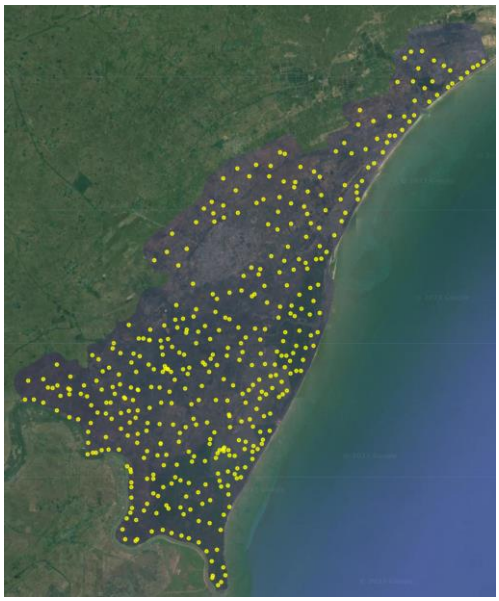

Fig. 5. Soil Sample points obtained from soil database

2.3. Selection of predictors and modeling

Because Machilipatnam lies in an arid zone [29], spectral indices are an efficient approach for detecting soil salinity in dry and semi-arid locations [11]. This study chose commonly used indicators of soil salinity to build a robust classification within the soil salinity model. The purpose is to examine and compare these indicators for subsequent refinement in selection. Fig. 6 provides an overview of selecting predictors and building a model.

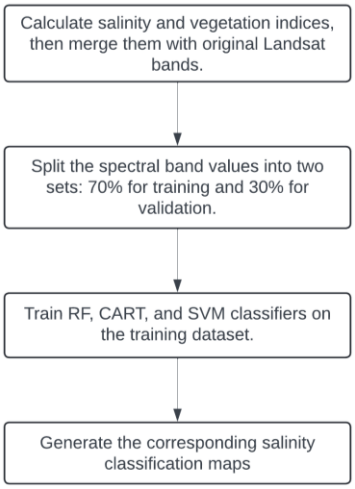

Fig. 6. Flowchart for selection of predictors and modeling

The study used Landsat 8 Operational Land Imager (OLI) (B2, B3, B4, B5, B6, B7) related to earth indicators. Table 1 shows various indices along with their formulas.

A function named *calculateSalinityIndices* was developed to compute 11 salinity indices and one vegetation index from a given Landsat image. Each index is derived by unique mathematical equations incorporating distinct spectral bands, such as near-infrared, red, green, and shortwave infrared. Using *ee.Image.expression*, the indices are computed, and *ee.Image.select* is used to link the bands with their names. These indices capture many aspects of the landscape's salinity characteristics. Then this function is applied to each image in the previously *corrected Landsat collection*, *correctedCollection*, using the map function, resulting in a new image collection named *salinityIndicesCollection*. This collection comprises the original Landsat bands combined with the newly calculated salinity indices, significantly enriching the dataset for subsequent analysis by providing valuable information related to soil salinity across the kharif seasons in the chosen study region. This stage is critical for acquiring a full understanding of salinity dynamics and potential impacts on agricultural regions.

Table 1. Salinity and vegetation indices of Landsat-8, along with their formulas

Index	Formula	Reference
SI1	$\frac{NIR}{SWIR1}$	
SI2	$\sqrt{G*R}$	[9]
SI3	$\sqrt{G^2+R^2+NIR^2}$	
SI4	$\sqrt{G^2+R^2}$	
SI5	$\frac{SWIR1}{SWIR2}$	[8]
SI6	$\frac{NIR-SWIR1}{NIR+SWIR1}$	
SI7	$\frac{SWIR1-SWIR2}{SWIR1+SWIR2}$	
SI8	$\frac{B}{R}$	[1]
SI9	$\frac{B-R}{B+R}$	[1]
NDSI	$\frac{R-NIR}{R+NIR}$	[19]
CRSI	$\sqrt{\frac{(NIR*R-G*B)}{(NIR*R+G*B)}}$	[28]
NDVI	$\frac{NIR-R}{NIR+R}$	[27]

The GEE script employs machine learning techniques to perform a thorough examination of soil salinity. To get ready for classification, additional processing is done on the salinity indices that were calculated from Landsat imagery and previously recorded in the *salinityIndicesCollection*. Using the median values, the script first condenses the collection into a single image. The computed salinity indices and particular spectral bands are then chosen by using *ee.Image.sampleRegions* to provide a dataset that is used to train and evaluate a RF classifier. The data is divided into training and validation sets, with 30% going toward validation and 70% going toward training. Using the training dataset, the RF classifier is trained considering variables like the bag fraction (0.6) using the *bagFraction* parameter and the number of trees (18) using the *numberOfTrees* parameter. To generate a salinity classification map, the trained classifier is applied to the complete collection of salinity indicators. The final map is viewed in the GEE map view and is colored to mark areas that are saline (red) and non-saline (green). Fig. 7 demonstrates the mapping of salt affected soils using RF.

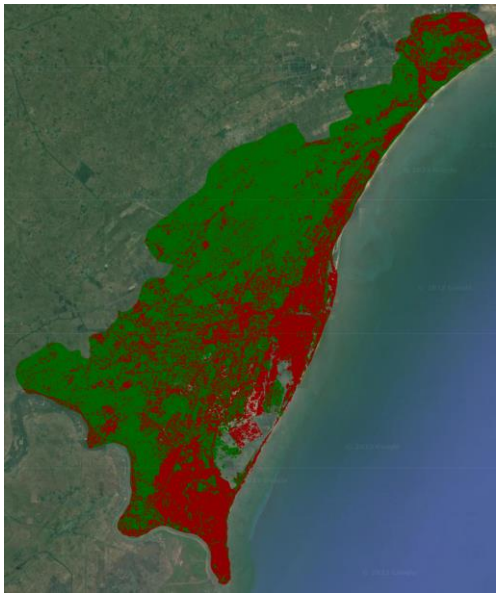

Fig. 7. Soil salinity map of Random Forest

ee.Feature(null,ee.Dictionary()) is used to retrieve the feature importance values of the developed RF model. To determine the relative significance of different spectral bands and salinity indices, get('importance')) is used. *ee.Image.sampleRegions*, *ee.ImageCollection.randomColumn*, *ee.Classifier.smileRandomForest*, and *ee.Image.classify* are among the GEE functions that are used to make the analysis, categorization, and interpretation of soil salinity patterns easier. For a complete analysis of the RF model's performance, confusion matrix computation and accuracy metrics are computed using *ee.Classifier.ConfusionMatrix*, *ee.ConfusionMatrix.accuracy*, and *ee.ConfusionMatrix.fscore*.

The pixel area for each classified region is then computed by adding a band of the classified cover to an image representing pixel areas. The *ee.Image.reduceRegion* function is performed to aggregate the pixel area information, grouping the data based on the salinity classification. The resulting aggregated data is then analyzed to obtain information about non-saline and saline areas. For each salinity class, the script calculates and formats the total area in square kilometers. The final output, stored in the variable result, is a dictionary outlining the extent of non-saline and saline areas within the study area, giving quantitative insights into the geographic distribution of soil salinity as determined by the RF classification.

The script implements the *ee.Classifier.smileCart* method to measure soil salinity, replicating the structure of the previously stated RF script. Initially, the CART classifier is trained using the provided training dataset, which comprises input attribute indices and salinity labels. The trained classifier is then applied to the complete collection of salinity indices, *salinityIndicesCollection*, resulting in the production of a salinity classification map called *cartClassified*. The CART mapping of SAS is shown in Fig. 8.

This map is visually depicted on the GEE map, with color distinctions for non-saline (green) and saline (red) areas. Feature importance values are extracted from the trained CART model, revealing insights into the significance of specific spectral bands and salinity indices for categorization. Confusion matrix computation and accuracy metrics are computed for a thorough examination of the CART model's performance. The script also calculates the areas within the research region that have been recognized as non-saline and saline, providing quantitative information about the geographical distribution of soil salinity based on the CART classification.

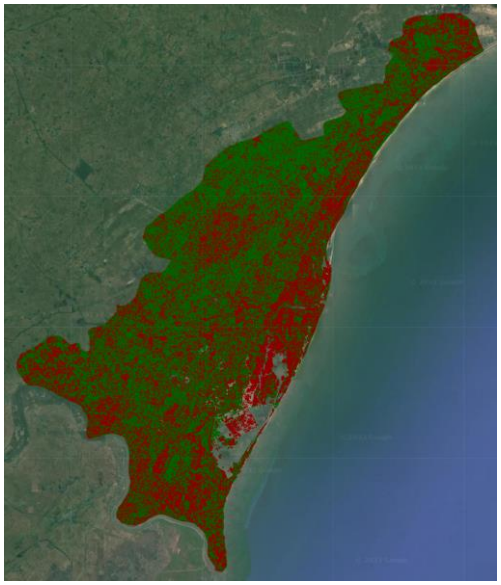

Fig. 8. Soil salinity map of Classification and Regression Trees

The script evaluates soil salinity using the *ee.Classifier.libsvm* method has a structure similar to the previously discussed RF and CART scripts. The SVM classifier is first trained using the specified training dataset, which includes input properties represented by indices and salinity labels. The trained SVM classifier is applied to the whole collection of salinity indices, yielding a salinity classification map termed *svmClassified*. This map is visualized on the GEE map, with different hues indicating non-saline (green) and saline (red) locations. The trained SVM model is used to derive feature importance values, which provide insight into the significance of various spectral bands and salinity indices for categorization. The script then computes confusion matrix metrics and accuracy measurements, allowing for a thorough evaluation of the SVM model's performance. The script calculates and displays the areas within the study area recognized as non-saline and saline, giving quantitative information on the geographic distribution of soil salinity based on the SVM classification. Fig. 9 depicts the mapping of SAS using SVM.

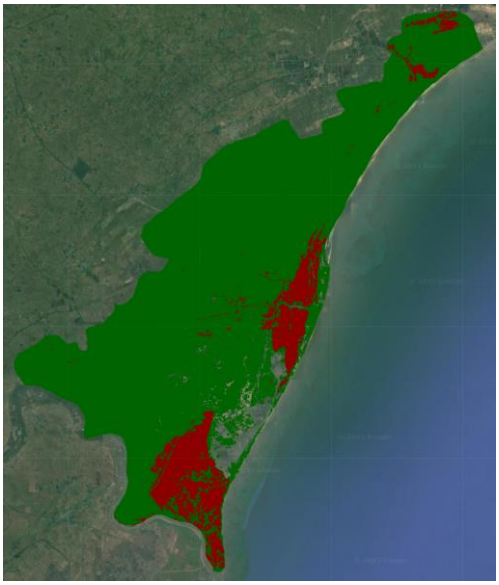

Fig. 9. Soil salinity map of Support Vector Machine

3. Results and discussion

The mean value of soil EC was obtained as 5.76 ds/m, with a range of 0.21 to 14.40 ds/m. 15.3% and 84.6% of the soil samples have EC values greater than 4 ds/m and less than 2 ds/m. The standard deviation of the soil samples was obtained as 3.25 ds/m. The hyperparameter was utilized to find the optimal number of trees as well as bag fraction. The RF model, obtained by giving 18 trees with a 0.6 bag fraction, had a maximum training accuracy of 91.8% and validation accuracy of 92.1%. Using the RF model, a variable of importance (VIMP) was derived. Twelve variables were used to train the RF model. The top 5 important factors were SI5, B2, B4, SI4, and SI1, and their VIMP scores were 8.94, 8.18, 8.04, 7.33, and 7.13 respectively. The maximum training accuracy of the CART model was 91.2% and the validation accuracy was 91.3%. B2, B4, B5, CRSI, and SI5 were the top five important factors, with VIMP scores of 4.75, 2.00, 1.10, 0.83, and 0.63, respectively. The SVM model's maximum training accuracy was 85.6% and validation accuracy was 86%. The top five essential factors were B2, B4, B5, CRSI, and SI5, with VIMP scores the same as the CART model. The total SAL calculated by the RF, CART, and SVM models is 134 km2, 134 km2, and 112 km2, respectively. Table. 2 contains the details regarding the performance metrics of the three machine learning models.

Table 2. Performance metrics of the Machine Learning models

Metrics	RF	CART	SVM
Accuracy (%)	92.17	91.30	86.00
Precision	0.93	0.87	0.78
Recall	0.92	0.94	0.91
F1-Score	0.92	0.90	0.94
SAL (Km^2)	134	134	112

4. Conclusion

SALs of various categories have been measured using advanced remote sensing and machine learning approaches when combined with field-level EC data. This study leveraged imagery data from Landsat-8 and applied various Machine Learning algorithms to discern between saline and non-saline soils. As input variables for the three machine learning models, various spectral indexes of vegetation and soil salinity were used. The RF model's hyperparameter was used to calculate the ideal number of trees and bag fraction to improve model accuracy. To map the salinity areas of soil accurately, high-resolution images are essential. Beyond salinity indices, spatial planning can offer a more comprehensive framework for future coastal management by combining predicted regional sea level rise, rainfall patterns, and land-use changes.

References

[1] Abbas A. et al.: Characterizing soil salinity in irrigated agriculture using a remote sensing approach. Physics and Chemistry of the Earth, Parts a/B/C 55–57, 2013, 43–52.
[2] Aksoy S. et al.: Assessing the performance of machine learning algorithms for soil salinity mapping in Google Earth Engine platform using Sentinel-2A and Landsat-8 OLI data. Advances in Space Research 2022.
[3] Asfaw E. et al.: Soil salinity modeling and mapping using remote sensing and GIS: The case of Wonji sugar cane irrigation farm, Ethiopia 17(3), 2018, 250–258.
[4] Bharathi S. et al.: Rainfall Analysis For Drought Investigation In Krishna Zone Of Andhra Pradesh. Agricultural Science Digest 31(2), 2011, 150–52.
[5] Cherlinka V.: Soil Salinization Causes & How to Prevent and Manage It. 2021 [https://eos.com/blog/soil-salinization/].
[6] Chhabra R.: Classification of Salt-Affected Soils. Arid Land Research and Management 19(1), 2004, 61–79.
[7] Chinchmalatpure A.: Reclamation and Management of Salt Affected Soils for Increasing Farm Productivity and Farmers' Income. 2017 [https://krishi.icar.gov.in/jspui/bitstream/123456789/10792/1/Reclamation%20and%20Management.pdf].
[8] CSSRI et al.: Indo-Dutch Network Project (IDNP): A Methodology for Identification of Water-logging and Soil Salinity Conditions Using Remote Sensing. 2002 [https://edepot.wur.nl/87639].
[9] Douaoui A. et al.: Detecting salinity hazards within a semiarid context by means of combining soil and remote-sensing data. Geoderma 134(1–2), 2006, 217–30.
[10] Extent and distribution of salt affected soils in India – ICAR-CSSRI: Central Soil Salinity Research Institute, 2024 [https://cssri.res.in/extent-and-distribution-of-salt-affected-soils-in-india/].
[11] Fathizad H. et al.: Investigation of the spatial and temporal variation of soil salinity using random forests in the central desert of Iran. Geoderma 365, 2020, 114233.
[12] Fathololoumi S. et al.: Improved digital soil mapping with multitemporal remotely sensed satellite data fusion: A case study in Iran. Science of the Total Environment 721, 2020, 137703.
[13] Gomes F. et al.: Velocidade de infiltração da água num plintossolo háplico de campo de murundu sob uma cronossequência de interferência antrópica. Revista Brasileira de Agricultura Irrigada 5(3), 2011, 245–253.
[14] Hoa P. et al.: Soil Salinity Mapping Using SAR Sentinel-1 Data and Advanced Machine Learning Algorithms: A Case Study at Ben Tre Province of the Mekong River Delta (Vietnam). Remote Sensing 11(2), 2019, 128.
[15] Hussain.: Present Scenario of Global Salt Affected Soils, Its Management and Importance of Salinity Research. International Research Journal of Biological Sciences 1–3, 2019, 1.
[16] Jabbar M. et al.: Assessment of Soil Salinity Risk on the Agricultural Area in Basrah Province, Iraq: Using Remote Sensing and GIS Techniques. Journal of Earth Science 23(6), 2012, 881–891.
[17] Kabiraj S. et al.: Automated delineation of salt-affected lands and their progress in coastal India using Google Earth Engine and machine learning techniques. Environmental Monitoring and Assessment 195(3), 2023.
[18] Kabiraj S. et al.: Comparative assessment of satellite images spectral characteristics in identifying the different levels of soil salinization using machine learning techniques in Google Earth Engine. Earth Science Informatics 15(4), 2022, 2275–2288.
[19] Khan N. et al.: Mapping Salt-affected Soils Using Remote Sensing Indicators-A Simple Approach with the Use of GIS IDRISI. 2001 [https://a-a-r-s.org/proceeding/ACRS2001/Papers/AGS-05.pdf].
[20] Krishna P.V. et al.: Health risk assessment of heavy metal accumulation in the food fish, Channa striata from Krishna river, Andhra Pradesh. International Journal of Fisheries and Aquatic Studies 9(2), 2021, 180–184.
[21] Kumar N. et al.: Remote Sensing and Machine Learning for Identification of Salt-affected Soils. Studies in Big Data 2021, 267–287.
[22] Kumar P. et al.: Soil Salinity and Food Security in India. Frontiers in Sustainable Food Systems 4, 2020.
[23] Madhu T. et al.: Mapping and Analysis of Wasteland in Machilipatnam Mandal, Krishna District, Andhra Pradesh, India by Using Geographical Information System. International Journal of Advanced Remote Sensing and GIS 4(1), 2015, 1435–1448.
[24] Mandal A.: Modern Tools and Techniques for Diagnosis and Prognosis of Salt Affected Soils and Poor-Quality Waters. Current Investigations in Agriculture and Current Research 2(5), 2018.
[25] Ramana Murty M. V. et al.: Monitoring of Coastal Geo-Environment for Hazard Mitigation: A Case Study of Machilipatnam Region, Andhra Pradesh, India. American Journal of Geospatial Technology 1(2), 2023, 27–38.
[26] Rani A. et al.: Identification of salt-affected soils using remote sensing data through random forest technique: a case study from India. Arabian Journal of Geosciences 15(5), 2022.
[27] Rouse J. W. et al.: Monitoring vegetation systems in the Great Plains with ERTS. NASA Special Publication 351, 1974, 309.
[28] Scudiero E. et al.: Remote sensing is a viable tool for mapping soil salinity in agricultural lands. California Agriculture 71(4), 2017, 231–38.
[29] Shankarnarayan K. A. et al.: Agroforestry in the arid zones of India. Agroforestry Systems 5(1), 1987, 69–88.
[30] Venkateshwarlu P. D. et al.: Marine Magnetic Indication of a Possible Submerged Volcano off Machilipatnam in Bay of Bengal. Journal of Geological Society of India 39, 1992, 197–203.
[31] Wang J. et al.: Capability of Sentinel-2 MSI data for monitoring and mapping of soil salinity in dry and wet seasons in the Ebinur Lake region, Xinjiang, China. Geoderma 353, 2019, 172–187.
[32] Wang J. et al.: Soil Salinity Mapping Using Machine Learning Algorithms with the Sentinel-2 MSI in Arid Areas, China. Remote Sensing 13(2), 2021, 305.
[33] Wu W. et al.: Soil salinity prediction and mapping by machine learning regression in Central Mesopotamia, Iraq. Land Degradation & Development 29(11), 2018, 4005–4014.
[34] Zhu S. et al.: Zeolite diagenesis and its control on petroleum reservoir quality of Permian in northwestern margin of Junggar Basin, China. Science China Earth Sciences 55(3), 2012, 386–396.

Prof. Govada Anuradha
e-mail: ganuradha@vrsiddhartha.ac.in

Dr. G Anuradha is currently working as an Associate Professor in the Department of Computer Science and Engineering, V. R. Siddhartha Engineering College, Vijayawada. She received a Ph.D. in Computer Science and Engineering in 2016 from Andhra University. She has 18 years of teaching experience. Her research interests lie in areas such as Data mining and Machine Learning. She published 10 papers in National and International journals.

https://orcid.org/0000-0002-0999-0376

Eng. Venkata Sai Sankara Vineeth Chivukula
e-mail: qualityhacker2002@gmail.com

Venkata Sai Sankara Vineeth Chivukula is a final year B.Tech student in Computer Science and Engineering at V. R. Siddhartha Engineering College, Vijayawada. He is passionate about Remote sensing, Machine learning, and Deep learning.

https://orcid.org/0009-0007-8919-599X

Eng. Naga Ganesh Kothagundla
e-mail: nagaganesh152@gmail.com

Naga Ganesh Kothagundla is a final year B.Tech student, specializing in Computer Science and Engineering at V. R. Siddhartha Engineering College, Vijayawada. He is interested in projects related to Machine learning, and Deep learning.

https://orcid.org/0009-0008-4830-726X